IEEE Access
Multidisciplinary | Rapid Review | Open Access Journal

Received October 25, 2021, accepted November 11, 2021, date of publication November 16, 2021,
date of current version November 29, 2021.

Digital Object Identifier 10.1109/ACCESS.2021.3128627

Dynamic Modeling and Eigen Analysis of Adjustable-Speed Pumped Storage Unit in Pumping Mode Under Power Regulation

ZHU ZHU[1,2], WENXIA PAN[1,3], TONGCHUI LIU[1,4], YE LI[1,5], AND MINGYANG LIU[6], (Member, IEEE)

[1]College of Energy and Electrical Engineering, Hohai University, Nanjing 210098, China
[2]College of Electrical Engineering, Tongling University, Tongling 244000, China
[3]Research Center for Renewable Energy Generation Engineering of Ministry of Education, Hohai University, Nanjing 210098, China
[4]State Grid Ningbo Power Supply Company, Ningbo 315200, China
[5]Powerchina Zhongnan Engineering Corporation Ltd., Changsha 410014, China
[6]State Grid Henan Electric Power Research Institute, Zhengzhou 450052, China

Corresponding author: Wenxia Pan (pwxhh@hhu.edu.cn)

This work was supported in part by the 111 Project of Renewable Energy and Smart Grid under Grant B14022 and in part by the Postgraduate Research and Practice Innovation Program of Jiangsu Province under Grant KYCX21_0475.

ABSTRACT The main merit of grid-connected adjustable-speed pumped storage unit (ASPSU) is the capability to control the pumping power flexibly, which contributes to active power balance in power system operation. Physics-based dynamic modeling of ASPSU in pumping mode under power regulation is the foundation of the quantitative analysis on its transient performance, which has been studied inadequately. This study aims to derive a dynamic model of ASPSU in pumping mode which embodies reversible pump-turbine characteristics, and to conduct eigen analysis on ASPSU in pumping mode which facilitates a better understanding of its intrinsic dynamics. Firstly, the dynamic model of reversible pump-turbine is revealed to depict its regulation properties that the pumping power is adjusted by rotational speed rather than guide vane opening. Then, the state-space representation of ASPSU in pumping mode is established to be utilized with small disturbances (including indicial and ramp tests) and validated by comparing simulated results with actual records of a commissioned ASPSU in Japan. It is also effective for compensating the wind power fluctuations based on a timescale of seconds in simulation. Finally, the eigenvalues, damping ratios, and participation factors of the state variables are investigated based on the small-signal-stability model of ASPSU in pumping mode under power regulation. The results of eigen analysis indicate that the small-signal behavior of the system is characterized by electromechanical mode and electromagnetic mode, and the latter is dominant. Moreover, the damping ratio of electromagnetic mode which is sensitive to system stability needs to be increased.

INDEX TERMS Adjustable-speed pumped storage unit (ASPSU), pumping mode, dynamic modeling, eigen analysis.

NOMENCLATURE

m	torque relative deviations [p.u.].
q	flow rate relative deviations [p.u.].
ω	rotational speed relative deviations [p.u.].
y	wicket gate opening relative deviations [p.u.].
h	water head relative deviations [p.u.].
e_ω	partial derivative of the torque with respect to rotational speed.
e_y	partial derivative of the torque with respect to wicket gate opening.
e_h	partial derivative of the torque with respect to water head.
$e_{q\omega}$	partial derivative of the flow with respect to rotational speed.
e_{qy}	partial derivative of the flow with respect to wicket gate opening.
e_{qh}	partial derivative of the flow with respect to water head.

The associate editor coordinating the review of this manuscript and approving it for publication was Ruisheng Diao.

M	mechanical torque [N · m].
M_R	rated mechanical torque [N · m].
Q	flow rate [m^3/s].
Q_R	rated flow rate [m^3/s].
w	rotational speed [rad/s].
w_R	rated rotational speed [rad/s].
Y	wicket gate opening [mm].
Y_R	rated wicket gate opening [mm].
H	water head [m].
H_R	rated water head [m].
T_w	water time constant [s].
η_p	pumping efficiency.
r	intermediate flow surface radius of outlet area [m].
β_0	runner intermediate flow surface angle [rad].
z	number of the guide vane.
r_a	intermediate flow surface effective outlet area [m].
g	gravitational acceleration, equals to 9.81 [m/s^2].
R_s, R_r	resistances of stator and rotor windings [p.u.].
L_s, L_r	self-inductances of stator and rotor windings [p.u.].
L_m	mutual inductance between stator and rotor windings [p.u.].
v_{sd}, v_{sq}	d, q-axis voltages of stator winding [p.u.].
v_{rd}, v_{rq}	d, q-axis voltages of rotor winding [p.u.].
i_{sd}, i_{sq}	d, q-axis currents of stator winding [p.u.].
i_{rd}, i_{rq}	d, q-axis currents of rotor winding [p.u.].
σ	leakage coefficient.
p	pole number.
ψ_{sd}, ψ_{sq}	d, q-axis magnetic fluxes of stator winding [p.u.].
P_s	real-time value of active power on stator winding [p.u.].
Q_s	real-time value of reactive power on stator winding [p.u.].
ψ_s	amplitude of magnetic flux of stator winding stator voltage.
$V_s\angle\varphi$	stator voltage.
ω_s	synchronous rotational speed [p.u.].
ω_m	rotational speed [p.u.].
T_J	inertia constant [s].
D_t	damping coefficient.
M_{em}	electromagnetic torque [p.u.].
M_p	mechanical torque [p.u.].
k_{p1}	proportional gain of the power adjuster.
k_{i1}	integral gain of the power adjuster [s^{-1}].
k_{p2}	proportional gain of the current adjuster.
k_{i2}	integral gain of the current adjuster [s^{-1}].
P_s^*	command value of active power on stator winding [p.u.].
Q_s^*	command value of reactive power on stator winding [p.u.].
x_1, x_2	intermediate variables.
x_3, x_4	intermediate variables.
s_r	slip frequency.
V	amplitude of the infinite bus voltage.
X_T, X_L	the reactances of the transformer and transmission line [p.u.].
X_{Tg}	reactance of the grid-side transformer [p.u.].

I. INTRODUCTION

Rocketing penetration of renewable energy sources with the intermittent nature into power system brings new challenges to active power balance. Large-scale energy storage facilities are effective solutions to meet these challenges, and the pumped storage plant is the major solution in terms of reliability and massive scale [1], [2]. The fixed-speed pumped storage unit has a constant runner speed due to directly connecting to the grid, and its pumping power cannot be properly adjusted in this regard. However, the adjustable-speed pumped storage unit (ASPSU) with a variable rotational speed typically has 30–40% power regulation range in pumping mode [3]–[5]. Therefore, it is vital and put into operation to establish the dynamic model and quantitatively analyze the power regulation characteristics of ASPSU in pumping mode.

ASPSU is usually composed of an alternating-current (AC) excitation induction machine and a reversible pump-turbine, as illustrated in Fig. 1 [6]. The reversible pump-turbine has adjustable guide vanes controlled by the speed governing system and fixed runner blades. In this way, two parts are mainly concentrated on in the dynamic modeling of ASPSU under power regulation. One is AC excitation induction machine and its controller [7]–[9], and the other is the reversible pump-turbine and associated governor [10], [11].

ASPSU under power regulation typically operates in two modes, that is, in turbine mode and in pumping mode. The reversible pump-turbine and associated governor operates differently in two modes. In details, the reversible pump-turbine is equivalent to a regular hydro-turbine when ASPSU runs in turbine mode, and it runs like a centrifugal pump when ASPSU runs in pumping mode [12]. From this perspective, the reversible pump-turbine and associated governor need to be carefully considered in dynamic modeling of ASPSU in different modes under power regulation.

The dynamic modeling of ASPSU in turbine mode has recently been investigated [11], [13], [14] and has also been considered in our previous study [10], while that in pumping mode has inadequately been studied. With respect to ASPSU model in pumping mode, some published results were obtained by neglecting the differences in regulation properties of the reversible pump-turbine between two modes, so the model of reversible pump-turbine and its controller in pumping mode was regarded as the same as that in turbine mode [15], [16]. Lung *et al.* introduced a simplified model of hydro-turbine and a model of associated governor for tuning guide vane opening in modeling of ASPSU in pumping mode [15]. Guo and Zhu established a linearized model of reversible pump-turbine and a model of its governor for adjusting guide vane aperture in modeling of ASPSU in

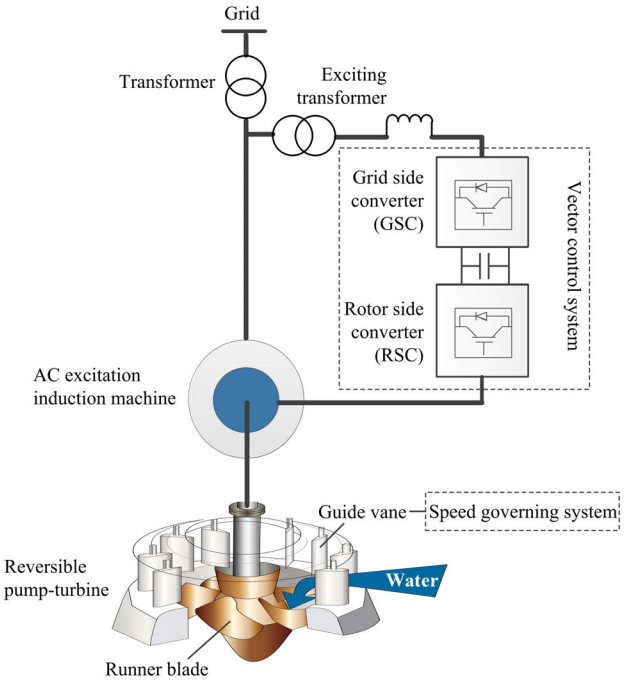

FIGURE 1. Typical schematic of ASPSU (figure modified from [6]).

pumping mode [16]. In fact, the input power of reversible pump-turbine in turbine mode is generally regulated by guide vane opening [3], [15], [17], [18], while its output power in pumping mode is adjusted by rotational speed rather than guide vane opening [5], [19]–[21]. Consequently, the model of reversible pump-turbine in turbine mode cannot be directly utilized in pumping mode, and the governor in turbine mode for tuning guide vane opening has no obvious effect on the adjustment of pumping power in this respect.

Following the fact that the pumping power of reversible pump-turbine is tuned by rotational speed rather than guide vane opening, some reports presented that the pumping power is proportional to the cube of the runner speed depending on the affinity law [5], [19]. But this law only explains the regulating principle of pumping power from a static perspective. There is no better way but to rely on empirical relationship when we determine the proportional coefficient in most cases [9].

Although some physics-based static models for ASPSU in pumping mode were derived [22], [23], they are unable to fully describe the dynamic behavior. So physics-based dynamic modeling of ASPSU in pumping mode under power regulation is still required for the simulation, the controller design, and the quantitative analysis on its transient performance. Pannatier *et al*. proposed a complicated hydraulic system model based on an electrical analogy, where pressure is analog to voltage and discharge is analog to current [24], [25], but the simulation is insufficient to compare results with the practical records. In summary, studies on the physics-based dynamic model of ASPSU in pumping mode under power regulation are meaningful, but still lacking yet.

Based on the dynamic modeling, the transient behavior of ASPSU in pumping mode under power regulation has been explored. The majority of published results were based on time-domain simulation which provides a depiction of the transient performance on ground of visual precision [18], [24], [25]. Nevertheless, they are unable to identify and quantify dynamic properties. These matching messages can be acquired with eigenvalues studies which have been insufficient so far.

This study aims to present the dynamic model of ASPSU in pumping mode which accurately describes reversible pump-turbine characteristics and to carry out eigen analysis on ASPSU in pumping mode. The main contributions and originality of this article are as follows: (1) The accurate model of reversible pump-turbine in pumping mode is established to shed light upon its regulation characteristics. (2) The physics-based dynamic model of ASPSU in pumping mode under power regulation is proposed and validated by comparing simulated results with practical records in indicial and ramp tests, respectively. This model is also effective for offsetting the wind power fluctuations based on a timescale of seconds in simulation. (3) The oscillation modes in this system are classified and discussed owing to eigen analysis.

The remaining of this paper is organized as follows: Section II performs the regulation properties of reversible pump-turbine in pumping mode and establishes its model according to this. Section III derives the mathematical model of ASPSU in pumping mode under power regulation and verifies its correctness. Section IV proposes the small-signal-stability model and accomplishes the eigen analysis. Section V condenses the main contributions and conclusions.

II. MODEL OF REVERSIBLE PUMP-TURBINE IN PUMPING MODE

A. CHARACTERISTICS

Reversible pump-turbine, a key physical component of ASPSU, is the most used in pumped storage plants [26]. Its characteristics stem from measurements on a reduced-scale model with certain speed $\upsilon = 0.2$ and demonstrate over the four quadrants in light of the IEC 60193 international standards, shown in Fig. 2 [25], [27]. N_{11}, Q_{11}, and M_{11} are factors often used in practical engineering ground on the speed N, the discharge Q, the torque M, the head H, and the reference diameter of the pump turbine D_{ref}, shown in formula (1).

$$N_{11} = \frac{N \cdot D_{ref}}{\sqrt{H}}, \quad Q_{11} = \frac{Q}{\sqrt{H} \cdot D_{ref}^2}, \quad M_{11} = \frac{M}{H \cdot D_{ref}^3} \tag{1}$$

The reversible pump-turbine commonly operates in steady state condition when the guide vane opening is over 50% (i.e., $y > 0.5$) [28], [29] in pump mode (i.e., $N_{11} < 0, Q_{11} < 0$, and $M_{11} > 0$) for meeting hydraulic characteristic requirements. In most circumstances, it operates at the rated point, point A shown in Fig. 2. Both speed and guide vane aperture can be

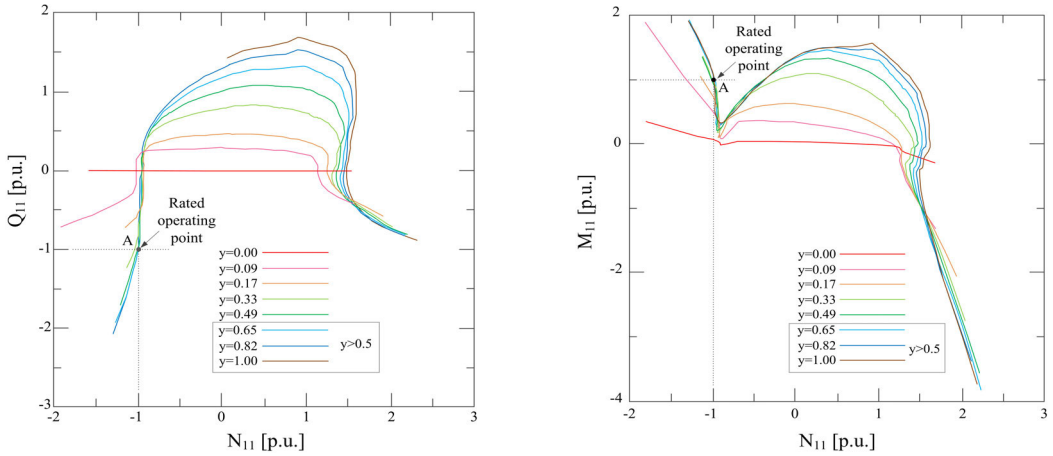

FIGURE 2. Reversible pump-turbine characteristics (figure modified from [24]).

controlled in reversible pump-turbine of ASPSU in the range of $N_{11} \in [0.9, 1.1]$ [2] and $y \in [0.5, 1.0]$. Fig. 2 shows that the guide vane opening has no obvious adjustment effect on the flow and torque in steady state condition in pumping mode. This proves the affinity law [5], [19] again that the torque could be tuned by speed instead of guide vane opening in this case.

B. MODEL

The linearized model of reversible pump-turbine applied to small operation variations is established on the basis of the standard six coefficient method, shown in formula (2) [30].

$$\begin{cases} m = e_\omega \omega + e_y y + e_h h \\ q = e_{q\omega} \omega + e_{qy} y + e_{qh} h \end{cases} \tag{2}$$

The six partial derivatives of the reversible pump-turbine are written in formula (3).

$$\begin{aligned} e_\omega &= \frac{\partial \left(M/M_R\right)}{\partial \left(w/w_R\right)} e_y = \frac{\partial \left(M/M_R\right)}{\partial \left(Y/Y_{\max}\right)} e_h = \frac{\partial \left(M/M_R\right)}{\partial \left(H/H_R\right)} \\ e_{q\omega} &= \frac{\partial \left(Q/Q_R\right)}{\partial \left(w/w_R\right)} e_{qy} = \frac{\partial \left(Q/Q_R\right)}{\partial \left(Y/Y_{\max}\right)} e_{qh} = \frac{\partial \left(Q/Q_R\right)}{\partial \left(H/H_R\right)} \end{aligned} \tag{3}$$

Formula (4) can be proposed owing to the reversible pump-turbine characteristics in pumping mode that the regulating guide vane aperture has no remarkable effect on the flow and torque. In this regard, the formula (2) can be rewritten in formula (5).

$$e_y \approx 0 \quad \text{and } e_{qy} \approx 0 \tag{4}$$

$$\begin{cases} m = e_\omega \omega + e_h h \\ q = e_{q\omega} \omega + e_{qh} h \end{cases} \tag{5}$$

The penstock system without significant influence by the elasticity of water and tube wall can be considered as rigid water hammer model, thus its dynamics can be described in formula (6) [31].

$$h = -T_w \dot{q} \tag{6}$$

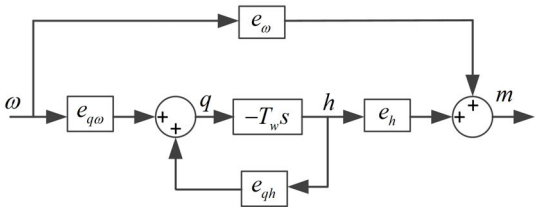

FIGURE 3. The block diagram of the reversible pump-turbine in pumping mode.

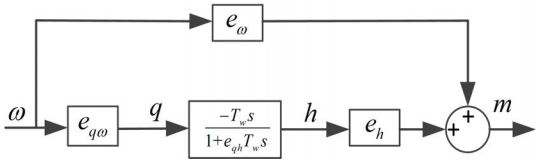

FIGURE 4. The equivalent block diagram of the reversible pump-turbine in pumping mode.

Therefore, the block diagram of the reversible pump-turbine in pumping mode can be demonstrated in Fig. 3, and equivalently expressed in Fig. 4. Meanwhile, the transient model of the reversible unit in pumping mode is given by formula (7)-(8).

$$\begin{aligned} G_p(s) &= \frac{m(s)}{\omega(s)} = e_\omega + e_{q\omega}\left(-\frac{T_w s}{1 + e_{qh} T_w s}\right) e_h \\ &= \frac{e_\omega - T_w s \left(e_{q\omega} e_h - e_{qh} e_\omega\right)}{1 + e_{qh} T_w s} \end{aligned} \tag{7}$$

$$M_p = M_{p0} + m \tag{8}$$

III. DYNAMIC MODEL OF ASPSU IN PUMPING MODE

A schematic diagram of ASPSU in pumping mode under power regulation is depicted in Fig. 5. ASPSU operates as a pump to store water from downstream reservoir to upstream one for converting electric energy into hydro energy. It is worth noting that ASPSU has breakthrough in pumping

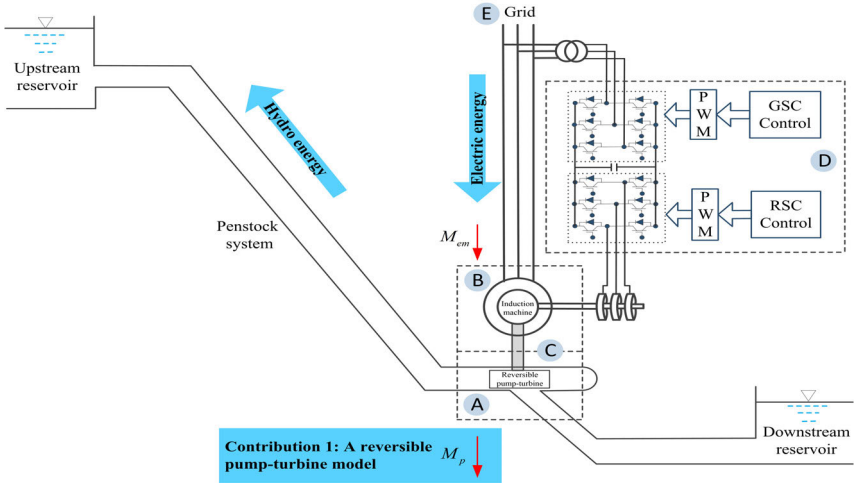

FIGURE 5. Schematic diagram of ASPSU in pumping mode under power regulation.

power adjustment under small disturbances because of having the ability to vary rotational speed [17], [18]. In this regard, the model of ASPSU in pumping mode for power regulation includes reversible pump-turbine Ⓐ, AC excitation induction Ⓑ drive train Ⓒ vector control system Ⓓ, and interface with power grid Ⓔ.

A. REVERSIBLE PUMP-TURBINE

The analytical expressions of transfer coefficients in the dynamic model of reversible pump-turbine in pumping mode are shown as [32]

$$\begin{cases} e_{q\omega} = \dfrac{a+1}{a-1-c}\dfrac{q_0}{\omega_0}, & e_{qh} = \dfrac{-1}{a-1-c}\dfrac{q_0}{h_0} \\ e_{\omega} = be_{q\omega} - \dfrac{m_0}{\omega_0}, & e_h = be_{qh} + \dfrac{m_0}{h_0} \end{cases} \tag{9}$$

where $a = (\eta_{p0}\omega_0^2/h_0)(r_a^2 w_R^2/gH_R)$; $b = (1-c)(m_0/q_0)$; $c = k^* Q_0/\eta_{p0}$; $q_0 = Q_0/Q_R$; $\omega_0 = w_0/w_R$; $h_0 = H_0/H_R$; $m_0 = M_0/M_R$; $r = D/2$; $\eta_{p0} = \rho g Q_0 H_0/M_0 w_0$; $r_a = r(1 - \pi \sin\beta_0/z)^{1/2}$. Subscripts R and 0 denote the rated condition and the steady condition, respectively. The range of r, β_0, and z are 1.80-2.10, 0-π/6, and 7-9, respectively [26].

A commissioned 400MW ASPSU in Ohkawachi power station, the most practical and valuable of the references reported [17], [18], is studied to get specific values of transfer coefficients. The results are $e_\omega = -3.590$, $e_h = 2.080$, $e_{q\omega} = -3.440$, and $e_{qh} = 1.670$ based on the operation parameters shown in Appendix A. Therefore, the reversible pump-turbine model for the typical case is illustrated in formula (10).

$$m(s) = \frac{-3.590 + 0.580s}{1 + 0.835s}\omega(s) \tag{10}$$

B. AC EXCITATION INDUCTION MACHINE

The state-space representation in the d-q reference frame is applied to AC excitation induction machine model, as described in equations (11)–(13), as shown at the bottom of the page, [10], [14].

The active power, reactive power, and electromagnetic torque on the stator winding are expressed in formula (14).

$$\begin{cases} P_s = \dfrac{3}{2}p\left(v_{ds}i_{ds} + v_{qs}i_{qs}\right) \\ Q_s = \dfrac{3}{2}p\left(v_{qs}i_{ds} - v_{ds}i_{qs}\right) \\ M_{em} = \dfrac{3L_m}{2L_s}p\left(\psi_{qs}i_{dr} - \psi_{ds}i_{qr}\right) = \dfrac{3}{2}pL_m \mathrm{Im}\left\{\vec{i}_s \cdot \vec{i}_r^*\right\} \end{cases} \tag{14}$$

$$\begin{bmatrix} \dot{i}_{ds} \\ \dot{i}_{qs} \\ \dot{i}_{dr} \\ \dot{i}_{qr} \end{bmatrix} = \left(\frac{1}{\sigma L_s L_r}\right) A_0 \begin{bmatrix} i_{ds} \\ i_{qs} \\ i_{dr} \\ i_{qr} \end{bmatrix} + \left(\frac{1}{\sigma L_s L_r}\right) \begin{pmatrix} L_r & 0 & -L_m & 0 \\ 0 & L_r & 0 & -L_m \\ -L_m & 0 & L_s & 0 \\ 0 & -L_m & 0 & L_s \end{pmatrix} \begin{bmatrix} v_{ds} \\ v_{qs} \\ v_{dr} \\ v_{qr} \end{bmatrix} \tag{11}$$

$$A_0 = \begin{pmatrix} -R_s L_r & \omega_m L_m^2 + \omega_s \sigma L_s L_r & R_r L_m & \omega_m L_m L_r \\ -\omega_m L_m^2 - \omega_s \sigma L_s L_r & -R_s L_r & -\omega_m L_m L_r & R_r L_m \\ R_s L_m & -\omega_m L_m L_s & -R_r L_s & -\omega_m L_s L_r + \omega_s \sigma L_s L_r \\ \omega_m L_m L_s & R_s L_m & \omega_m L_s L_r - \omega_s \sigma L_s L_r & -R_r L_s \end{pmatrix} \tag{12}$$

$$\sigma = 1 - L_m^2 \Big/ L_s L_r \tag{13}$$

When the stator flux direction is aligned with d-axis in the d-q reference frame, we have formula (15).

$$\begin{cases} \psi_{ds} = \psi_s = -V_s/\omega_s \\ \psi_{qs} = 0 \end{cases} \tag{15}$$

When p equals to 1, formula (16) is obtained by substituting (15) into (14).

$$\begin{cases} P_s = -\dfrac{3L_m}{2L_s} V_s i_{qr} \\ Q_s = \dfrac{3V_s^2}{2\omega_s L_s} - \dfrac{3V_s L_m}{2L_s} i_{dr} \\ M_{em} = \dfrac{3}{2} L_m \left(i_{qs} i_{dr} - i_{ds} i_{qr}\right) = -\dfrac{3L_m}{2L_s\omega_s} V_s i_{qr} \end{cases} \tag{16}$$

C. DRIVE TRAIN

The drive train system is usually seen as a series of rigid bodies linked by massless shafts in the modeling of power system. The one-mass model is used for on-grid ASPSU, since the drive train runs as a single equivalent mass with nearly equal participation of all inertias [14], [15]. The swing of ASPSU is given by equation (17).

$$\frac{T_J}{p}\dot{\omega}_m = M_p - M_{em} - D_t \Delta\omega_m \tag{17}$$

When p equals to 1 and D_t equals to zero, equation (17) can be simplified as equation (18).

$$\dot{\omega}_m = \frac{1}{T_J}\left(M_p - M_{em}\right) \tag{18}$$

D. ROTOR SIDE CONVERTER (RSC) CONTROL

The active power regulation of AC excitation induction machine is mainly controlled by RSC control [17], [18], so only RSC control model is mentioned when ignoring the dynamics of grid side converter (GSC) control. The block diagram of RSC control is demonstrated in Fig. 6, and its equation is written as [33].

$$\begin{cases} \dot{x}_1 = P_s^* - P_s \\ \dot{x}_2 = k_{p1}\left(P_s^* - P_s\right) + k_{i1}x_1 - i_{qr} \\ \dot{x}_3 = Q_s^* - Q_s \\ \dot{x}_4 = k_{p1}\left(Q_s^* - Q_s\right) + k_{i1}x_3 - i_{dr} \end{cases} \tag{19}$$

$$\begin{cases} v_{qr} = k_{p2}\left(k_{p1}(P_s^* - P_s) + k_{i1}x_1 - i_{qr}\right) \\ \qquad + k_{i2}x_2 + \omega_s s_r L_m i_{ds} + \omega_s s_r L_{rr} i_{dr} \\ v_{dr} = k_{p2}\left(k_{p1}\left(Q_s^* - Q_s\right) + k_{i1}x_3 - i_{dr}\right) \\ \qquad + k_{i2}x_4 - \omega_s s_r L_m i_{qs} - \omega_s s_r L_{rr} i_{qr} \end{cases} \tag{20}$$

where $s_r = 1 - \omega_m/\omega_s$; $L_{rr} = L_r + L_m$.

E. INTERFACE WITH POWER GRID

The interface with power grid, shown in Fig. 7, is expressed as (21)-(22) [34], [35]

$$\begin{bmatrix} v_{ds} \\ v_{qs} \end{bmatrix} = \begin{bmatrix} \cos\varphi \\ -\sin\varphi \end{bmatrix} V - \begin{bmatrix} 0 & -X_{TL} \\ X_{TL} & 0 \end{bmatrix}$$

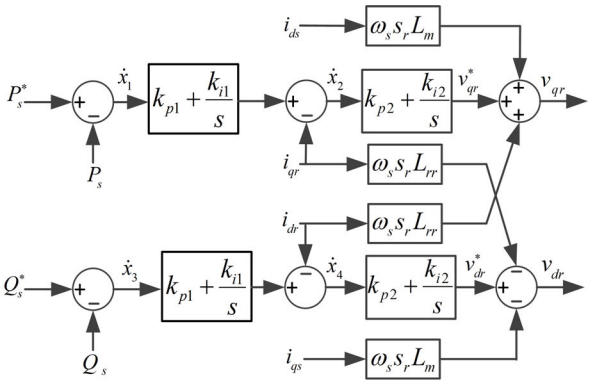

FIGURE 6. Block diagram of RSC control.

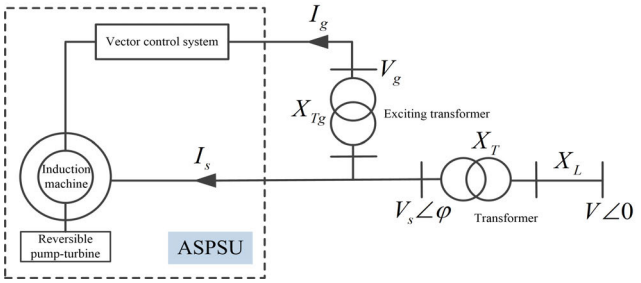

FIGURE 7. The interface with power network (figure modified from [35]).

$$\times \left(\begin{bmatrix} i_{ds} \\ i_{qs} \end{bmatrix} + \begin{bmatrix} i_{dg} \\ i_{qg} \end{bmatrix}\right) \tag{21}$$

$$\begin{bmatrix} v_{ds} \\ v_{qs} \end{bmatrix} - \begin{bmatrix} v_{dg} \\ v_{qg} \end{bmatrix} = \begin{bmatrix} 0 & -X_{Tg} \\ X_{Tg} & 0 \end{bmatrix} \begin{bmatrix} i_{dg} \\ i_{qg} \end{bmatrix} \tag{22}$$

where $X_{TL} = X_T + X_L$.

Significantly, the expression of the converter topologies can be ignored. It must be considered when studying on fault behavior or high oscillation process with very frequent switching, while it can be neglected when researching on slow transient performance such as power perturbation in this work [14]. From this perspective, different common converter topologies (cycloconverter, back-to-back converter, and matrix converter) have no influence on the model of ASPSU in pumping mode.

F. MODEL VALIDATION

The PSCAD/EMTDC software is utilized to build the dynamic model of ASPSU in pumping mode derived for time-domain simulation. The rated specifications of 400MW ASPSU commissioned in Ohkawachi power station are listed in Appendix B, and simulated parameters are given in Appendix C. There are three steps in model validation as follows. In *Step 1*, indicial and ramp tests are simulated for comparing simulated results with actual records. In *Step 2*, step tests with different signal amplitudes are simulated for testing the power regulation range of the model. In *Step 3*, they are simulated that dynamic performances of ASPSU

for compensating the wind power fluctuations based on a timescale of seconds.

Step 1: Indicial and ramp tests

The practical operations are performed as follows, and Table 1 gives some operation parameters. When it comes to the indicial test, the recorded running time of the on-grid ASPSU is 83s. The power command is step increased by 0.195p.u. at t_1, and step decreased at t_2. Starting from t_1, power input fast reacts within 0.2s, and rotational speed climbs up during 12s. Beginning with t_2, power input also rapidly reacts within 0.2s, and runner speed climbs down during 12s.

TABLE 1. Some operation parameters of ASPSU in pumping mode.

The indicial test		The ramp test			
t_1	t_2	t_3	t_4	t_5	t_6
14s	44s	27s	34s	47s	54s

When it comes to the ramp test, the measured running time is the same. The power command is ramped up by 0.385p.u. from t_3 to t_4, and ramped down from t_5 to t_6. At the stage of rising, power input fast follows the command and speed climbs up within 12s. At the stage of falling, power input also quickly follows the signal, and speed climbs down during 12s.

Simulated results of ASPSU in pumping mode in two tests are demonstrated in Fig. 8 and Fig. 9, respectively. Corresponding measurements, being tried to keep exactly as those reported in [3], are also shown in each figure for comparison. Note that the actual records are shown in nominal values in [3], but are converted into per unit ones with consideration for easily comparing with those employed in simulation.

According to comparisons in measurements and simulation results showcased in Fig. 8 and Fig. 9, it can be found that:

(1) The simulated terminal voltage amplitudes nearly remain constant, the same as on-site measurements in both indicial and ramp tests. The vector control adopted in ASPSU makes it possible to control active power and reactive power independently, and the reactive power is kept balance during active power regulation process. So the terminal voltage amplitudes which are determined by reactive power balance keep the same.

(2) There is no description of wicket gate opening dynamics in simulation, while it is recorded in practice. Wicket gate opening has not been taken into account in the dynamic model of ASPSU in pumping mode under regulation regarding the fact that adjusting guide vane opening has no remarkable effect on power regulation. The guide vane opening still exists in practical operation records possibly due to optimizing the efficiency of ASPSU in pumping mode by tuning the guide vane when the speed varies [25]. This optimization process itself is not modeled, and the optimal relationships are usually supplied by the manufacturer [17].

(3) Simulated speed dynamics are similar to actual records in two tests. The differences in the minimum/maximum speed

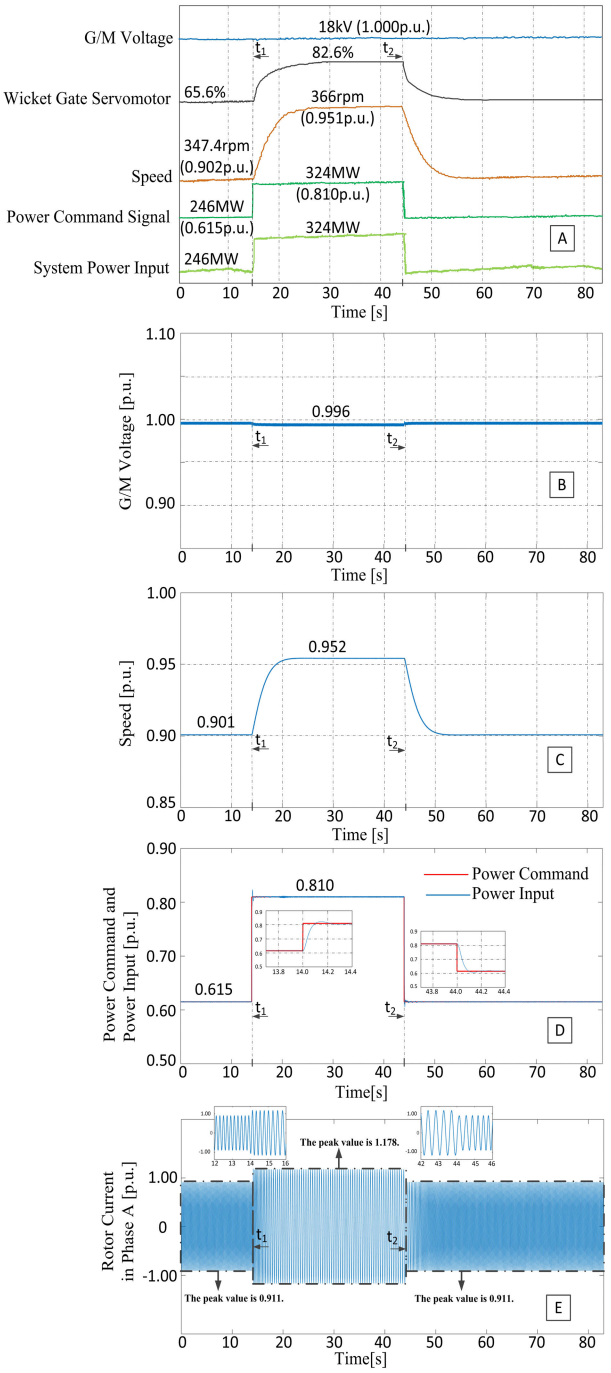

FIGURE 8. Measurements and simulated results of ASPSU in pumping mode in indicial test: (A) Measurements [3], (B) Simulated voltage, (C) Simulated speed, (D) Simulated power command and power input, (E) Simulated rotor current in phase A.

values are no more than 0.3%, listed in Table 2. Moreover, the settling time of speed (12s) is much longer than that of power input (0.2s) in indicial test, and the settling time of speed is a little longer than that of power input (within 5s) in ramp test both due to the inertia constant of ASPSU.

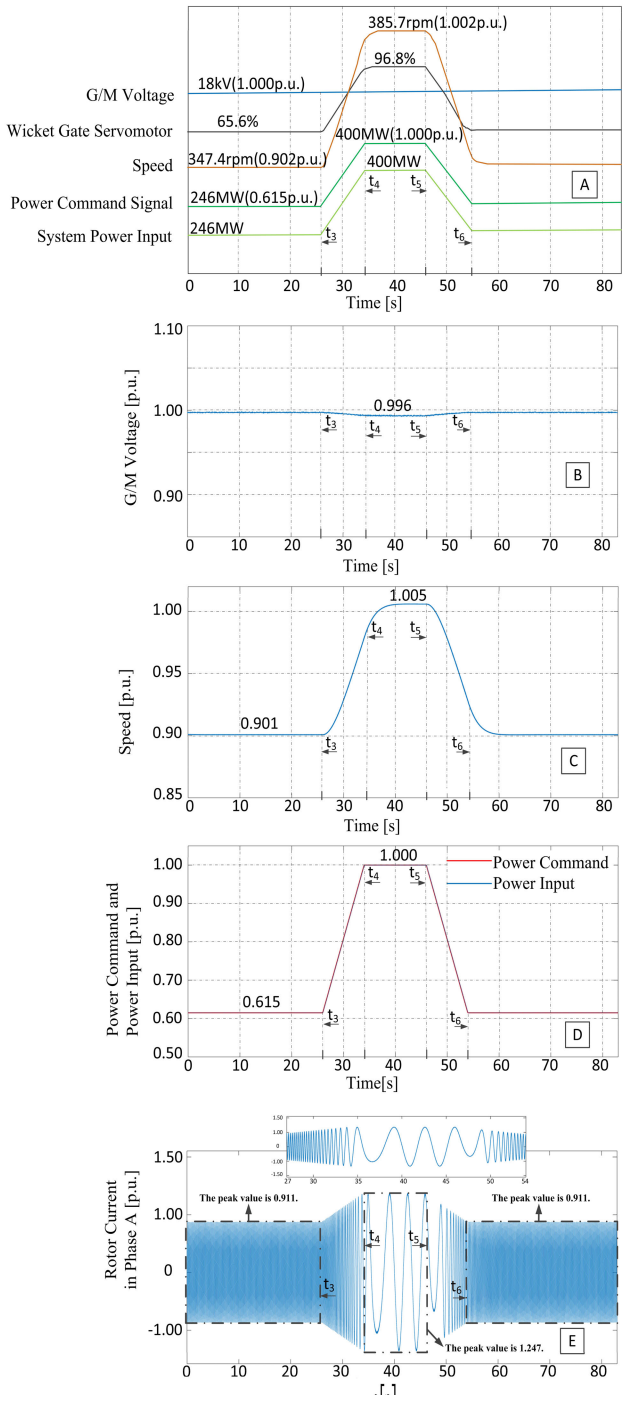

FIGURE 9. Measurements and simulated results of ASPSU in pumping mode in ramp test: (A) Measurements [3], (B) Simulated voltage, (C) Simulated speed, (D) Simulated power command and power input, (E) Simulated rotor current in phase A.

(4) Simulated power input dynamics agree with actual records in both indicial and ramp responses. Fast response of power input is acquired owing to rapid changes in both amplitude and phase of rotor current by the vector control.

Step 2: Pumping power regulation range tests

Considering ASPSU typically has 30–40% power regulation range in pumping mode [3]–[5], the pumping power regulation range of the model proposed is tested by 10%, 20%, 30%, and 40% in order under step power commands with different magnitudes. The simulated results are presented in Fig. 10.

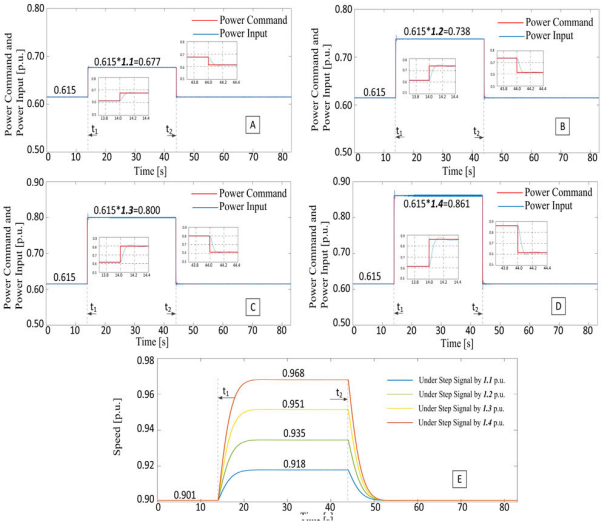

FIGURE 10. Simulated results of ASPSU in pumping power regulation range tests: (A) Simulated power command and power input under step signal by 1.1 p.u., (B) Simulated power command and power input under step signal by 1.2 p.u., (C) Simulated power command and power input under step signal by 1.3 p.u., (D) Simulated power command and power input under step signal by 1.4 p.u., (E) Simulated speeds under different step signals.

According to simulation results shown in Fig. 10, it can be found that:

(1) The model proposed can achieve 40% regulation range in pumping power with 7.44% ((0.968-0.901)/0.901 = 7.44%) regulation range in runner speed.

(2) The settling time of both power input and speed cannot be changed under different step disturbances. But the maximum speed increases with the increase of disturbance magnitude.

Step 3: Compensating the wind power fluctuations tests

Being determined 40% regulation range in pumping power, the model is examined whether being able to offsetting the wind power fluctuations or not in wind farm-grid integration system. Motivated by [14], the power references in consideration of the wind power fluctuations are input as setpoints of active power of ASPSU in pumping mode. These wind power fluctuations based on a timescale of seconds are obtained from the spectrum characteristics of wind speed fluctuations recorded in a typical wind farm over times utilizing the fast Fourier transform (FFT) algorithm [36]. The wind farm power fluctuations within 40s are shown Fig. 11, and the fluctuation range is 0.067p.u.-0.166p.u. Note that the records are shown in nominal values in [36], but are converted into

TABLE 2. Comparisons in speed dynamics of measurements and simulated results.

	Characteristics	Measurements	Simulated results	Differences
Indicial response by 0.195pu	Minimum speed	0.902p.u.	0.901p.u.	0.1%
	Maximum speed	0.951p.u.	0.952p.u.	0.1%
Ramp response by 0.385pu	Minimum speed	0.902p.u.	0.901p.u.	0.1%
	Maximum speed	1.002p.u.	1.005p.u.	0.3%

Where *difference*=|((*measurement*)–(*simulated result*))/(*measurement*)|

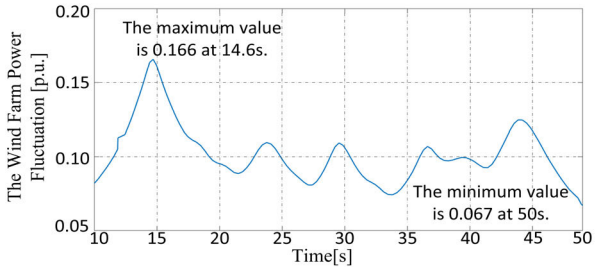

FIGURE 11. The wind farm power fluctuation (figure modified from [36]).

per unit ones in view of keeping the same as those in fore-mentioned tests.

Before 10s, ASPSU in pumping mode operates at steady state, the same as that in fore-mentioned tests (power input equals to 246MW/0.615p.u., speed equals to 347.4rpm/0.901p.u.). Starting from 10s, ASPSU operates under the wind power fluctuations. The dynamic behaviors are showcased in Fig. 12.

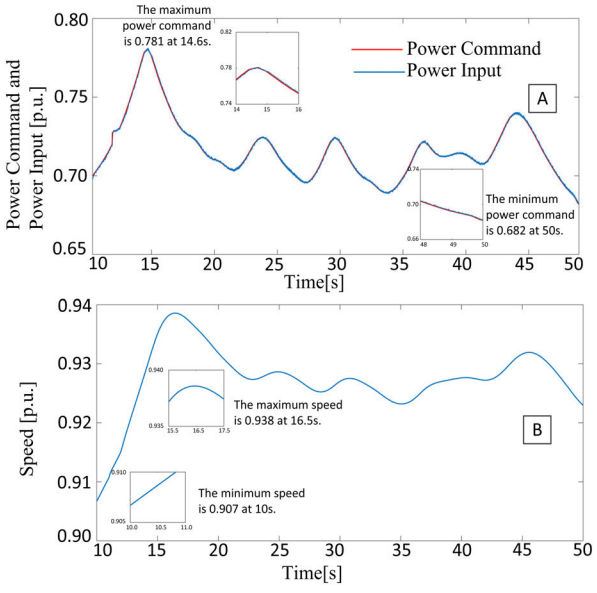

FIGURE 12. Simulated results of ASPSU in pumping mode under wind farm power fluctuations: (A) Simulated power command and power input, (B) Simulated speed.

According to simulation results shown in Fig. 12, it can be seen that:

(1) The model proposed is effective for offsetting wind power fluctuations within 40s. Fast response of power input is acquired in hundred milliseconds owing to the vector control.

(2) The response time of speed is slower than that of power input (16.5-14.6 = 1.9s), which possibly causes the minimum speed and the minimum power to appear at different times.

In summary, the simulation results in *Step 1* achieve an agreement with the on-site measurements to validate the model of on-grid ASPSU in pumping mode under power regulation since characteristics (voltage, speed, active power, and rotor current) have been correctly considered in anticipated model. The simulation results in *Step 2* and *Step 3* show that the model proposed can achieve 40% regulation range in pumping power and can be utilized for compensating the wind power fluctuations.

IV. EIGEN ANALYSIS OF ASPSU IN PUMPING MODE

Dynamic model of ASPSU in pumping mode commonly makes it possible to implement eigen analysis on it. A small-signal stability model, the linear model in the neighbourhood of an initial equilibrium operation point, is usually employed for eigen analysis.

A. SMALL-SIGNAL-STABILITY MODEL

Firstly, the mathematical model of ASPSU in pumping mode can be described as a set of differential algebraic equations, shown as

$$\begin{cases} \dot{x} = f(x, u) \\ y = g(x, u) \end{cases} \tag{23}$$

where x, u, and y are state variables, input variables, and output variables, respectively; f and g are the vectors of differential and algebraic equations.

In this study, $x = \left[\omega_m, m, x_1, x_2, x_3, x_4, i_{ds}, i_{qs}, i_{dr}, i_{qr}\right]^T$; $u = \left[P_s^*, Q_s^*, V_s, \varphi\right]^T$; $y = \left[v_{dr}, v_{qr}, v_{dg}, v_{qg}\right]^T$; f are included in (10)-(13), (16), and (18)-(19); g are included in (20)-(22).

Then, the initial state operation point (power input equals to 246MW, speed equals to 347.4rpm) is seen as an initial equilibrium operation point where all the deviations are

TABLE 3. The eigenvalues, damping ratios, participation factors, and modes labeling of ASPSU in pumping mode.

$\lambda=\sigma\pm j\omega$	σ	ω	f	T	ζ	ASV1	ASV2	Mode
$\lambda_{1,2}$	−16.28	12.57rad/s	2.00Hz	0.50s	0.79	ω_m	m	Electromechanical mode
$\lambda_{3,4}$	−5.68	102.80rad/s	16.37Hz	0.06s	0.05	i_{qr}	i_{dr}	Electromagnetic mode
λ_5	−30.92	/	/	/	1.00	x_3	x_4	Non-oscillation mode
λ_6	−34.01	/	/	/	1.00	x_4	x_3	
λ_7	−0.67	/	/	/	1.00	x_1	i_{qr}	
λ_8	−0.66	/	/	/	1.00	x_2	i_{dr}	

simultaneously zero, given by equation (24).

$$\begin{cases} \dot{x} = f(x_0, u_0) = 0 \\ y_0 = g(x_0, u_0) \end{cases} \tag{24}$$

In addition, formula (23) is linearized by a Taylor series expansion around (x_0, u_0). Without consideration of the terms of order two and above, the linearized model is written as

$$\begin{cases} \Delta\dot{x} = A\Delta x + B\Delta u \\ \Delta y = C\Delta x + D\Delta u \end{cases} \tag{25}$$

where n, m, and r are the dimensions of the state vector, the output vector, and the input vector, respectively. The size of matrices: A (10 × 10), B (10 × 4), C (4 × 10), D (4 × 4).

$$A = \begin{bmatrix} \frac{\partial f_1}{\partial x_1} & \cdots & \frac{\partial f_1}{\partial x_n} \\ \cdots & & \cdots \\ \frac{\partial f_n}{\partial x_1} & \cdots & \frac{\partial f_n}{\partial x_n} \end{bmatrix}; \quad B = \begin{bmatrix} \frac{\partial f_1}{\partial u_1} & \cdots & \frac{\partial f_1}{\partial u_r} \\ \cdots & & \cdots \\ \frac{\partial f_n}{\partial u_1} & \cdots & \frac{\partial f_n}{\partial u_r} \end{bmatrix};$$

$$C = \begin{bmatrix} \frac{\partial g_1}{\partial x_1} & \cdots & \frac{\partial g_1}{\partial x_n} \\ \cdots & & \cdots \\ \frac{\partial g_m}{\partial x_1} & \cdots & \frac{\partial g_m}{\partial x_n} \end{bmatrix}; \quad D = \begin{bmatrix} \frac{\partial g_1}{\partial u_1} & \cdots & \frac{\partial g_1}{\partial u_r} \\ \cdots & & \cdots \\ \frac{\partial g_m}{\partial u_1} & \cdots & \frac{\partial g_r}{\partial u_r} \end{bmatrix}.$$

Finally, the system state matrix A_{sys} is acquired in formula (26) [33], [37].

$$\begin{cases} \Delta\dot{x} = A_{sys}\Delta x \\ A_{sys} = \left[A - BD^{-1}C\right] \end{cases} \tag{26}$$

The stator current dynamics can be neglected because the stator currents are considered as algebraic variables due to its corresponding mode having a small time constant [34], [35], [38], [39]. The reduced small-signal stability model is given by formula (27) in this regard, and A'_{sys} is an 8 × 8 square matrix.

$$\Delta\dot{x}' = A'_{sys}\Delta x' \tag{27}$$

It can be observed from the analytical expression of A'_{sys} that:

(1) The dynamics of speed and mechanical torque of ASPSU in pumping mode cannot be tuned by the converter control gains if there is no independent control for the speed.

(2) The dynamics of rotor current and intermediate variables of ASPSU in pumping mode can be regulated by converter control parameters.

B. EIGEN ANALYSIS

As discussed above, the eigenvalues of A'_{sys} which determine the modes of ASPSU in pumping mode are related to the control parameters, but it is difficult to acquire the analytical equations of eigenvalues involving the control gains expressions. The control parameters need to be selected for eigen analysis in this regard.

They are main considerations that induction machine specifications, pulse-width modulation (PWM) switching frequency, filter parameters, and equivalent controller type when designing the control gains [40], [41], and they are selected as $[k_{p1}, k_{p2}, k_{i1}, k_{i2}] = [1.1, 10.0, 34.0\text{s}^{-1}, 6.7\text{s}^{-1}]$ in this study.

The oscillation frequency f_i, damping ratio ζ_i, and participation factors p_{ki} for the eigenvalues $\lambda_i = \sigma_i \pm j\omega_i$ $(i \in 1, 2, \ldots, 8)$ can be calculated as

$$\begin{cases} f_i = \omega_i/2\pi \\ \zeta_i = -\sigma_i \Big/ \sqrt{\sigma_i^2 + \omega_i^2} \\ p_{ki} = \phi_{ki}\psi_{ik} \end{cases} \tag{28}$$

where ϕ_{ki} is kth entry of the right eigenvector ϕ_i; Ψ_{ik} is kth entry of the left eigenvector Ψ_i.

The p_{ki} is the participation of the kth state variable in the ith eigenvalues, and the state variables having two highest participation factors in the corresponding eigenvalues are denoted as ASV1 and ASV2 [34], [35].

The eigenvalues, damping ratios, participation factors, and modes labeling are listed in Table 3, and it can be found that:

(1) According to Lyapunov's first method, the system of ASPSU in pumping mode for power regulation is stable because all eigenvalues have negative real parts.

(2) There are three stable modes, two of which are oscillating. Two oscillation modes in this system are electromechanical and electromagnetic modes according to definition and classification of power system stability in IEEE PES TR-77 technical report [42] if neglecting the stator current dynamics in power regulation. The slower mode, oscillating at 2.00Hz, is electromechanical mode related to rotor speed dynamics. The faster mode, oscillating at 16.37Hz, is electromagnetic mode related to rotor current dynamics.

(3) The electromagnetic mode is dominant due to having smaller absolute value of the real part ($5.68 < 16.28$). Meanwhile, it has the insufficient damping ratio (0.05), which needs an in-depth improvement from a stability point view.

At the initial stage of stability analysis on ASPSU in pumping mode under power regulation, assuming that the pumping power is adjusted by guide vane opening, Guo and Zhu introduced that PI governor gains and water time constant have significant influence on the stability of ASPSU based on Hopf bifurcation theory [16]. Assuming that the pumping power is adjusted by guide vane opening, Gao *et al.* presented that PI governor gains and vector control parameters have effect on the stability of ASPSU based on Hopf bifurcation theory [43]. When following the fact that the pumping power is adjusted by rotational speed instead of guide vane opening, the system stability depends on vector control parameters as the detailed analysis above. From this perspective, different modeling methods reveal different main influence factors on the system stability.

V. CONCLUSION

Having great performance on active power regulation, on-grid ASPSU in pumping mode has attracted world-wide attention. Accurate physics-based dynamic modeling of ASPSU in pumping mode which is indispensable for the simulation, the controller design, and the quantitative analysis on its transient behaviors has been insufficient yet. This paper has presented a validated dynamic model of ASPSU in pumping mode which quantitatively describing its regulation properties that the pumping power is adjusted by rotational speed rather than guide vane opening. This model is also the foundation of further stability analysis on ASPSU in pumping mode under power regulation. The main findings of this study are as follows:

(1) The reversible pump-turbine of ASPSU in pumping mode has two control variables (guide vane aperture and runner speed), but its pumping power is adjusted by rotational speed rather than guide vane opening. This study proposes a dynamic generic model of reversible pump-turbine in pumping mode which quantitatively depicts this regulation properties and its specific model for a commissioned ASPSU in Japan. The generic model/the specific model can be used as a form of user defined reversible pump-turbine for simulating the ASPSU dynamics in pumping mode.

(2) Based on the model of the reversible pump-turbine proposed, this study derives a physics-based dynamic model of ASPSU in pumping mode with no independent control for the speed. With the derived model, simulation of dynamic performance with small disturbance is ready to conduct. On one hand, the proposed model of ASPSU in pumping mode under power regulation is first validated in both indicial and ramp tests. On the other hand, the proposed model's regulation range of pumping power and the proposed model's ability of compensating the wind power fluctuations are tested.

(3) Generally speaking, eigen analysis of ASPSU in pumping mode can be carried out only when its state-space representation is obtained. Based on the modeling technique including the inherent control model of ASPSU in pumping mode proposed, this study presents its eigen analysis used by an eighth-order small-signal stability model. The small-signal behavior is characterized by two modes, electromechanical mode associated with rotor speed dynamics and electromagnetic mode associated with rotor current dynamics. The latter is the dominated one, and its damping ratio which is sensitive to system stability needs to be developed.

In the end, this study could be extended in two aspects as follows: (1) In terms of in-depth stability analysis on ASPSU in pumping mode under power regulation, the scheme for increasing the damping ratio of the electromagnetic mode can be considered. (2) Based on the model of ASPSU in pumping mode derived in this work, the multi-energy hybrid system (pumped storage with ASPSU, wind, and solar) can be explored from the perspective of frequency stability.

APPENDIX A
OPERATION PARAMETERS OF A COMMISSIONED 400MW ASPSU IN OHKAWACHI POWER STATION

According to the pump mode operation range of ASPSU of Ohkawachi power station shown in Fig. 13 [3], the ASPSU operates in rated condition at point A, and in steady condition at point B. The corresponding operation parameters are showcased in Table 4. The pumping efficiency can be seen as constant by using the efficiency optimization function in the ASPSU in Ohkawachi power station [3]. Meanwhile, the pumping efficiency of ASPSU is generally around

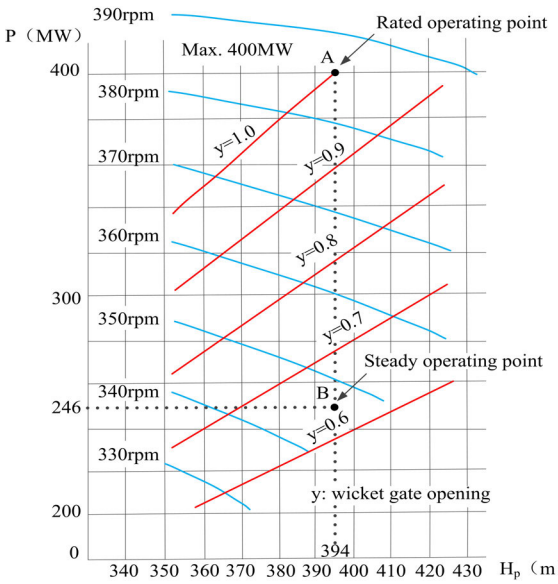

FIGURE 13. Pump mode operation range of ASPSU of Ohkawachi power station (figure modified from [3]).

TABLE 4. The operation parameters of ASPSU of Ohkawachi power station.

	Power input P	Speed	Water head H_p
Rated operating point A	400.0MW	385.0rpm	394.0m
Steady operating point B	246.0MW	347.4rpm	394.0m

0.9 although its value of the specific case has not been published yet. So it is treated as a constant of 0.9 for simplicity and without loss of generality in this paper [4], [22].

APPENDIX B
RATED SPECIFICATIONS OF A COMMISSIONED 400MW ASPSU IN OHKAWACHI POWER STATION IN PUMPING MODE [3]

TABLE 5. The rated specifications of a ASPSU in Ohkawachi power station in pumping mode.

No.	Rated specifications	
01	Maximum system input	400MW
02	Pump mode rated power factor	1
03	Speed range	330~390rpm
04	Generator terminal voltage	18kV
05	Rated cycloconverter capacity	72MVA
06	Rated cycloconverter voltage	5.2kV

APPENDIX C
MODEL PARAMETERS [10], [14]

TABLE 6. The model parameters.

No.	Model specifications	
01	Inertia constant T_J	11s
02	Resistance of the stator winding R_s	0.0115p.u.
03	Resistance of the rotor winding R_r	0.0128p.u.
04	Self-inductance of the stator winding L_s	1.3p.u.
05	Self-inductance of the rotor winding L_r	1.3p.u.
06	Mutual inductance L_m	3.475p.u.

REFERENCES

[1] M. S. Guney and Y. Tepe, "Classification and assessment of energy storage systems," *Renew. Sustain. Energy Rev.*, vol. 75, pp. 1187–1197, Aug. 2017.
[2] S. Rehman, L. M. Al-Hadhrami, and M. M. Alam, "Pumped hydro energy storage system: A technological review," *Renew. Sustain. Energy Rev.*, vol. 44, pp. 586–598, Apr. 2015.
[3] T. Kuwabara, A. Shibuya, H. Furuta, E. Kita, and K. Mitsuhashi, "Design and dynamic response characteristics of 400 MW adjustable speed pumped storage unit for Ohkawachi power station," *IEEE Trans. Energy Convers.*, vol. 11, no. 2, pp. 376–384, Jun. 1996.
[4] M. Valavi and A. Nysveen, "Variable-speed operation of hydropower plants: A look at the past, present, and future," *IEEE Ind. Appl. Mag.*, vol. 24, no. 5, pp. 18–27, Sep. 2018.
[5] M. Alizadeh Bidgoli, W. Yang, and A. Ahmadian, "DFIM versus synchronous machine for variable speed pumped storage hydropower plants: A comparative evaluation of technical performance," *Renew. Energy*, vol. 159, pp. 72–86, Oct. 2020.
[6] E. Muljadi, M. Singh, V. Gevorgian, M. Mohanpurkar, R. Hovsapian, and V. Koritarov, "Dynamic modeling of adjustable-speed pumped storage hydropower plant," in *Proc. IEEE Power Energy Soc. Gen. Meeting*, Denver, CO, USA, Jul. 2015, pp. 1–5.
[7] A. Joseph and T. R. Chelliah, "A review of power electronic converters for variable speed pumped storage plants: Configurations, operational challenges, and future scopes," *IEEE Trans. Emerg. Sel. Topics Power Electron.*, vol. 6, no. 1, pp. 103–119, Mar. 2018.
[8] L. Ji, J. Sun, M. Zhou, and W. Tian, "AC excitation control strategy of variable speed pumped storage units based on active disturbance rejection control," *J. Eng.*, vol. 2017, no. 13, pp. 1195–1199, Jan. 2017.
[9] K. R. Vasudevan, V. K. Ramachandaramurthy, G. Venugopal, J. B. Ekanayake, and S. K. Tiong, "Variable speed pumped hydro storage: A review of converters, controls and energy management strategies," *Renew. Sustain. Energy Rev.*, vol. 135, Jan. 2021, Art. no. 110156.
[10] W. Pan, Z. Zhu, T. Liu, M. Liu, and W. Tian, "Optimal control for speed governing system of on-grid adjustable-speed pumped storage unit aimed at transient performance improvement," *IEEE Access*, vol. 9, pp. 40445–40457, 2021.
[11] J. I. Sarasúa, J. I. Pérez-Díaz, J. R. Wilhelmi, and J. Á. Sánchez-Fernández, "Dynamic response and governor tuning of a long penstock pumped-storage hydropower plant equipped with a pump-turbine and a doubly fed induction generator," *Energy Convers. Manage.*, vol. 106, pp. 151–164, Dec. 2015.
[12] J. Raabe, *Hydro Power: The Design, Use, and Function of Hydromechanical, Hydraulic, and Electrical Equipment*. 1st ed. Düsseldorf, Germany: VDI Verlag, 1985.
[13] Y. Chen, C. Deng, and Y. Zhao, "Coordination control between excitation and hydraulic system during mode conversion of variable speed pumped storage unit," *IEEE Trans. Power Electron.*, vol. 36, no. 9, pp. 10171–10185, Sep. 2021.
[14] W. Yang and J. Yang, "Advantage of variable-speed pumped storage plants for mitigating wind power variations: Integrated modelling and performance assessment," *Appl. Energy*, vol. 237, pp. 720–732, Mar. 2019.
[15] J. K. Lung, Y. Lu, W. L. Hung, and W. S. Kao, "Modeling and dynamic simulations of doubly fed adjustable-speed pumped storage units," *IEEE Trans. Energy Convers.*, vol. 22, no. 2, pp. 250–258, Jun. 2007.
[16] W. Guo and D. Zhu, "Nonlinear modeling and operation stability of variable speed pumped storage power station," *Energy Sci. Eng.*, vol. 9, no. 10, pp. 1703–1718, Jul. 2021.
[17] J. Feltes, Y. Kazachkov, and B. Gong, "Modeling adjustable speed pumped storage hydro units employing doubly-fed induction machines," Argonne Nat. Lab., Lemont, IL, USA, Tech. Rep. ANL/DIS-13/06, 2013.
[18] V. Koritarov, T. Veselka, J. Gasper, B. Bethke, A. Botterud, J. H. Wang, M. Mahalik, Z. Zhou, and C. Milostan, "Modeling and analysis of value of advanced pumped storage hydropower in the United States," Argonne Nat. Lab., Lemont, IL, USA, Tech. Rep. ANL/DIS-14/07, 2014.
[19] T. Ahonen, J. Tamminen, J. Ahola, and J. Kestila, "Frequency-converter-based hybrid estimation method for the centrifugal pump operational state," *IEEE Trans. Ind. Electron.*, vol. 59, no. 12, pp. 4803–4809, Dec. 2012.
[20] T. Mercier, M. Olivier, and E. Dejaeger, "Operation ranges and dynamic capabilities of variable-speed pumped-storage hydropower," *J. Phys., Conf. Ser.*, vol. 813, Apr. 2017, Art. no. 012004.
[21] C. Moreira, N. Fulgêncio, B. Silva, C. Nicolet, and A. Béguin, "Identification of dynamic simulation models for variable speed pumped storage power plants," *J. Phys., Conf. Ser.*, vol. 813, Apr. 2017, Art. no. 012006.
[22] J. Liang and R. G. Harley, "Pumped storage hydro-plant models for system transient and long-term dynamic studies," in *Proc. IEEE PES Gen. Meeting*, Minneapolis, MN, USA, Jul. 2010, pp. 1–8.
[23] W. Yao, C. Deng, and P. Peng, "Optimization method and reduced-order steady-state model for variable-speed pump-turbine unit," *IEEE Access*, vol. 9, pp. 31130–31142, 2021.
[24] Y. Pannatier, C. Nicolet, B. Kawkabani, J. L. Deniau, A. Schwery, F. Avellan, and J. J. Simond, "Transient behavior of variable speed pump-turbine units," in *Proc. 24th Symp. Hydraulic Mach. Syst.*, Foz do Iguaçu, Brazil, Jan. 2008, pp. 1–14.
[25] Y. Pannatier, B. Kawkabani, C. Nicolet, J. J. Simond, A. Schwery, and P. Allenbach, "Investigation of control strategies for variable-speed pump-turbine units by using a simplified model of the converters," *IEEE Trans. Ind. Electron.*, vol. 57, no. 9, pp. 3039–3049, Sep. 2010.
[26] Y. M. Lu and J. Z. Pan, *Pumped Storage Plants*. Beijing, China: Water Resources and Electric Power Press, 1992.
[27] *Storage Pumps and Pump-Turbines-Model Acceptance Tests*, Standard IEC 60193, 1999.
[28] Z. Zuo and S. Liu, "Flow-induced instabilities in pump-turbines in China," *Engineering*, vol. 3, no. 4, pp. 504–511, Aug. 2017.
[29] D. Li, Z. Zuo, H. Wang, S. Liu, X. Wei, and D. Qin, "Review of positive slopes on pump performance characteristics of pump-turbines," *Renew. Sustain. Energy Rev.*, vol. 112, pp. 901–916, Sep. 2019.

[30] H. Fang, L. Chen, N. Dlakavu, and Z. Shen, "Basic modeling and simulation tool for analysis of hydraulic transients in hydroelectric power plants," *IEEE Trans. Energy Convers.*, vol. 23, no. 3, pp. 834–841, Sep. 2008.
[31] H. Zhang, D. Chen, B. Xu, and F. Wang, "Nonlinear modeling and dynamic analysis of hydro-turbine governing system in the process of load rejection transient," *Energy Convers. Manage.*, vol. 90, pp. 128–137, Jan. 2015.
[32] L. Wang, Q. Han, D. Chen, C. Wu, and X. Wang, "Non-linear modelling and stability analysis of the PTGS at pump mode," *IET Renew. Power Gener.*, vol. 11, no. 6, pp. 827–836, May 2017.
[33] R. Quan and W. X. Pan, "A low-order system frequency response model for DFIG distributed wind power generation systems based on small signal analysis," *Energies*, vol. 10, no. 5, p. 657, May 2017.
[34] P. Kundur, *Power System Stability and Control*. New York, NY, USA: McGraw-Hill, 1994.
[35] F. Wu, X. P. Zhang, K. Godfrey, and P. Ju, "Small signal stability analysis and optimal control of a wind turbine with doubly fed induction generator," *IET Gener., Transmiss. Distrib.*, vol. 1, no. 5, pp. 751–760, Sep. 2007.
[36] M. X. Han, G. T. Bitew, S. A. Mekonnen, and W. Yan, "Wind power fluctuation compensation by variable speed pumped storage plant in a grid integrated system: Frequency spectrum analysis," *CSEE J. Power Energy Syst.*, vol. 7, no. 2, pp. 381–395, Mar. 2021.
[37] L. Yang, G. Y. Yang, Z. Xu, Z. Y. Dong, K. P. Wong, and X. Ma, "Optimal controller design of a doubly-fed induction generator wind turbine system for small signal stability enhancement," *IET Gener., Transmiss. Distrib.*, vol. 4, no. 5, p. 579, 2010.
[38] F. Mei and B. Pal, "Modal analysis of grid-connected doubly fed induction generators," *IEEE Trans. Energy Convers.*, vol. 22, no. 3, pp. 728–736, Sep. 2007.
[39] P. Ledesma and J. Usaola, "Effect of neglecting stator transients in doubly fed induction generators models," *IEEE Trans. Energy Convers.*, vol. 19, no. 2, pp. 459–461, Jun. 2004.
[40] G. Bitew, M. Han, S. Mekonnen, and P. Simiyu, "A variable speed pumped storage system based on droop-fed vector control strategy for grid frequency and AC-bus voltage stability," *Electronics*, vol. 7, no. 7, p. 108, Jul. 2018.
[41] X. Zhang, "Study on the PWM rectifier and its control strategies," Ph.D. dissertation, Dept. Electr. Eng., Hefei Univ. Technol., Hefei, China, 2003.
[42] N. Hatziargyriou, J. V. Milanović, C. Rahmann, V. Ajjarapu, C. Cañizares, I. Erlich, D. Hill, I. Hiskens, I. Kamwa, B. Pal, P. Pourbeik, J. J. Sanchez-Gasca, A. Stanković, T. Van Cutsem, V. Vittal, and C. Vournas, "Stability definitions and characterization of dynamic behavior in systems with high penetration of power electronic interfaced technologies," IEEE Power Syst. Dyn. Perform. Committee, Washington, DC, USA, Tech. Rep. IEEE PES TR-77, 2020.
[43] C. Gao, X. Yu, H. Nan, C. Men, P. Zhao, Q. Cai, and J. Fu, "Stability and dynamic analysis of doubly-fed variable speed pump turbine governing system based on Hopf bifurcation theory," *Renew. Energy*, vol. 175, pp. 568–579, Sep. 2021.

ZHU ZHU received the B.S. degree in electrical engineering from the North China University of Water Resources and Electric Power, Zhengzhou, China, in 2010, and the M.S. degree in photovoltaic and renewable energy engineering from the University of New South Wales (UNSW), Sydney, Australia, in 2011. She is currently pursuing the Ph.D. degree in electrical engineering with Hohai University, Nanjing, China. She is also a Science Researcher in Tongling University. Her main research interest includes renewable energy generation technology.

WENXIA PAN received the B.S. and M.S. degrees from Wuhan University, Wuhan, China, in 1982 and 1987, respectively, and the Ph.D. degree from Hohai University, Nanjing, China, in 2004. She is currently a Professor of electrical engineering with Hohai University. She has published two research books. She has authored or coauthored over 100 journal articles. Her current research interests include renewable energy generation systems and high-voltage and insulation technology.

TONGCHUI LIU received the B.S. degree from Xuchang University, in 2012, and the M.S. degree from Hohai University, Nanjing, China, in 2015, where he is currently pursuing the Ph.D. degree in electrical engineering. He is an Electrical Engineer with State Grid Ningbo Power Supply Company, Ningbo, China. His main research interest includes renewable energy generation technology.

YE LI received the B.S. degree in electrical engineering from Hohai University, Nanjing, China, in 2018, where he is currently pursuing the M.S. degree in electrical engineering. He is also a staff in Powerchina Zhongnan Engineering Corporation Ltd., Changsha, China. His main research interest includes renewable energy generation technology.

MINGYANG LIU (Member, IEEE) received the B.S. degree in electrical engineering from the North China University of Water Resources and Electric Power, Zhengzhou, China, in 2013, and the Ph.D. degree in electrical engineering from Hohai University, Nanjing, China, in 2019. He is currently an Electrical Engineer with the State Grid Henan Electric Power Research Institute, Zhengzhou. His research interests include power systems analysis and wind power generation.